Vol 17 No 7, July 2008
1674-1056/2008/17(07)/2655-07

Chinese Physics B

© 2008 Chin. Phys. Soc.
and IOP Publishing Ltd

Effect of the stoichiometry on the electronic structure of the Ni(111)/α-Al_2O_3(0001) interface: a first-principles investigation*

Shi Si-Qi(施思齐)[a)b)†], Tanaka Shingo (田中真悟)[b)], and Kohyama Masanori(香山正憲)[b)]

[a)] *Department of Physics, Center for Optoelectronics Materials and Devices, Zhejiang Sci-Tech University, Xiasha College Park, Hangzhou* 310018, *China*

[b)] *Materials Science Research Group, Research Institute for Ubiquitous Energy Devices, National Institute of Advanced Industrial Science and Technology,* 1-8-31, *Midorigaoka, Ikeda, Osaka* 563-8577, *Japan*

(Received 20 May 2007; revised manuscript received 2 November 2007)

In this paper first-principles calculations of Ni(111)/α-Al_2O_3(0001) interfaces have been performed, and are compared with the preceding results of the Cu (111)/α-Al_2O_3(0001) interface [2004 *Phil. Mag. Lett.* **84** 425]. The Al-terminated and O-terminated interfaces have quite different adhesion mechanisms, which are similar to the Cu(111)/α-Al_2O_3(0001) interface. For the O-terminated interface, the adhesion is caused by the strong O-2p/Ni-3d orbital hybridization and ionic interactions. On the other hand, the adhesion nature of the Al-terminated interface is the image-like electrostatic and Ni–Al hybridization interactions, the latter is substantial and cannot be neglected. Charge transfer occurs from Al_2O_3 to Ni, which is opposite to that in the O-terminated interface. The charge transfer direction for the Al-terminated and O-terminated Ni(111)/α-Al_2O_3(0001) interfaces is similar to that in the corresponding Cu(111)/α-Al_2O_3(0001) interface, but there exist the larger charge transfer quantity and consequent stronger adhesion nature, respectively.

Keywords: metal/ceramic interface, stoichiometry, electronic structure, first-principles calculations
PACC: 6848, 6480E, 7115A

1. Introduction

Alumina is one of the most thoroughly studied important oxide crystals for its wide applications in catalysts, electronic packaging and high-temperature structural ceramic.[1−3] It is crucial for such electronic and structural applications to fabricate metal/alumina interface with desirable electronic, optical, mechanical and thermal properties. This metal/ceramic interface may play a role in materials failure of current combustion engine thermal barrier coatings (TBCs). A large number of experiments have been performed for the metal/Al_2O_3 system because metal or metal-containing alloys are often used for applications.[4−13]

On the theoretical side, there have also been many studies about the adhesion, atomic and electronic structures of the metal/Al_2O_3 interfaces[14−25] and other interfaces or grain boundaries.[26−30] However, it should be noted that, before 1990, *ab initio* work investigating metal/alumina was mainly limited to small clusters of alumina with one or more metal atoms, calculation was often reduced without considering the model closer to that used in the experiment.[22−25] Only until recently, some theoretical studies indicated that the bonding nature of metal/alumina interfaces seems to depend greatly on the interface stoichiometry.[15−20] Thus, from a more fundamental standpoint, these interfaces are interesting simply because they are poorly characterized and their intrinsic nature at the atomic level is not understood thoroughly.

In the present work, we concentrate on the Ni(111)/α-Al_2O_3(0001) interface. We deal with both O-terminated (O-rich) and Al-terminated (stoichiometric) interfaces in order to examine the O–Ni and

*Project supported by Qianjiang Talent Project of Zhejiang Province of China (Grant No 2007R10028), the Science Foundation of Zhejiang Sci-Tech University (ZSTU) in China (Grant No 0613271-Y), and Science Foundation of Zhejiang Province of China (Grant No Y407188).

†E-mail: siqishi@yahoo.com, siqishi@zstu.edu.cn

Al–Ni interactions, respectively. We use a first-principles pseudopotential method based on the density functional theory (DFT), and obtain the stable atomic configuration, adhesive energies and electronic properties of the interfaces. In addition, the present results are compared with our preceding calculations of the O-terminated and Al-terminated Cu(111)/α-Al_2O_3(0001) interfaces.[20] By the way, it is emphasized that the first-principle method is very important in the field of basic studies of metal/ceramic interfaces. Interfaces between more ionic solids and noble or simple metals such as Ag/MgO or Al/MgO systems are often non-reactive experimentally, *ab initio* calculations of such interfaces[31−33] have shown that the adhesion mainly originates from the electrostatic interactions, which partially justify the traditional image interaction model. On the other hand, if metals have transitions with reactive d orbitals, there should exist the covalent interactions such as orbital hybridization predicted by *ab initio* calculations of Nb/Al_2O_3[34] and Cu/Al_2O_3 interfaces.[20] However, the classic image interaction model cannot deal directly with orbital hybridization and charge transfer at the interface, both of which can be investigated from the first-principles method.

2. Theoretical method

We employ the standard pseudopotential total energy method based on the DFT within the local density approximation (LDA).[35] The wave functions are obtained by solving the Kohn–Sham equation using a plane wave basis. The electronic ground state is efficiently obtained via parallel computations[36] by using the 'residual minimization/direct inversion in the iterative subspace' (RMM-DIIS) method coupled with the effective Pulay charge-mixing scheme.[37,38] Optimized norm-conserving pseudopotentials[39] are used in the separable form[40] with a plane-wave cut-off energy of 120Ry, which is large enough for the present system. Four and nine sampling k-points within the irreducible Brillouin zone of the present supercell are used for self-consistent calculations and final band-structure calculations, respectively. The stable configuration is obtained by static relaxation according to the Hellmann–Feynman forces till the maximum force is smaller than 0.5 eV/nm.

We focus on an ideal coherent interface by expanding Ni(111) planes as other *ab initio* calculations of the same system.[14,19−21] As mentioned in the previous work, there also exist three types of interface models according to the site of the interface Ni atom on the hexagonal unit cell of an Al_2O_3(0001) plane.[19,20] Here, we examine the O-site model in detail, where the interface Ni atoms are situated above the surface O atoms, because this is the most stable one for the Al-terminated systems in our test as well as in Ref.[19]. Although the O-site model for the O-terminated systems is not the most stable, it is rather similar to that for the Al-terminated systems, except for the removal of surface Al atoms. As a result, the more direct comparison between two interfaces can be performed.

The present supercell is constructed by the periodical piling of an Al_2O_3 (0001) slab and a Ni slab with five Ni (111) layers. The Al_2O_3 slab contains four oxygen atomic layers and eight aluminium atomic layers for the Al-terminated case or six aluminium atomic layers for the O-terminated case. On each (0001) or (111) atomic layer, one Al, three O or three Ni atoms belong to the unit cell. The stable interface configuration is determined through the total-energy minimization by iterating the relaxation for different supercell lengths in the direction normal to the interface. In each relaxation step, the C_{3i} symmetric property is preserved, which keeps the two interfaces in the supercell identical to each other.

After obtaining the stable configuration, the work of separation, $W_{\rm sep}$, is calculated. This is the energy consumption per unit area in separating an interface into two fixed separate surfaces with the same atomic positions as the interface. Next, each separate surface is relaxed into a free surface to obtain the adhesion energy, $W_{\rm ad}$, which is the energy gain per unit area in forming the stable interface from two relaxed free surfaces.

3. Results and discussion

Table 1 lists the calculated values of $W_{\rm ad}$ and $W_{\rm sep}$ for O-terminated and Al-terminated interfaces together with other available theoretical and experimental ones. In this table, it is found that the calculated $W_{\rm ad}$ for Al-terminated Ni/Al_2O_3 interface is 1.828 J/m^2, which is much larger than that (1.30J/m^2) given by Zhang *et al.*[19] This is very similar to the case that the $W_{\rm ad}$ (1.27J/m^2) for Al-terminated Cu/Al_2O_3 interface, as calculated in our

previous work, is much larger than the corresponding one (0.58J/m^2) given by Zhang *et al.*[19] It should be mentioned that, for the Al-terminated Cu/Al_2O_3 interface, Batyrev and Kleinman[21] used the calculation scheme and obtained the W_{ad} similar to those presented in our previous work. On the other hand, it generally considers that the LDA somewhat overestimates surface energies. Thus, the large difference between the present value and that given by Zhang *et al* [19] using Generalized Gradient Approximation (GGA) seems to be comprehensible, although Batyrev and Kleinman[21] did not report the W_{ad} of Ni/Al_2O_3 interface.

Table 1. Work of separation, W_{sep}, and work of adhesion, W_{ad}, for the Ni(111)/Al_2O_3(0001) interfaces. Results of the Cu(111)/Al_2O_3(0001) interface (Ref.[20]) are also listed.

	W_{sep}/(J/m^2)	W_{ad}/(J/m^2)
Ni(111)/Al_2O_3(0001) interface		
O-terminated	7.178	7.051
Al-terminated	2.387	1.828
theoretical		1.30[a]
experimental		1.17[b], 1.114[c]
Cu(111)/Al_2O_3(0001) interface		
O-terminated		6.96
Al-terminated	1.62	1.27

[a]Ref.[19], [b]Ref.[41], [c]Ref.[7]

W_{sep} and W_{ad} of the O-terminated interface are quite larger than those of the Al-terminated interface, as shown in Table 1. This suggests that the former has much stronger adhesion bonding than the latter. The same tendency was observed for Cu/Al_2O_3.[20] As the preliminary analysis, we can examine the respective interfacial stoichiometry. The Al_2O_3(0001) surface, which is used for producing the O-terminated interface, is not stoichiometric, i.e., surface Al atoms are removed. Therefore, it seems to be intuitional that there exists the strong bonding between the interfacial Ni and O atoms to saturate the bare O dangling bonds. However, the Al-terminated interface is stoichiometric, where the Al_2O_3(0001) surface is chemically stable. Hence it seems that the interfacial Ni atoms cannot interact strongly with Al_2O_3. It is interesting that, even in this case, there exists the hybridization interaction between the interfacial Ni and Al atoms, as will be discussed below. This rather big difference can be thoroughly understood from the following analysis of charge density and density of states. Thus it seems that the absence of the interface Al atom strengthens the interfacial adhesion significantly.

For the O-terminated and Al-terminated interfaces, their W_{ad} are lower than the respective W_{sep} due to performing the relaxation for the Al_2O_3 and Ni surfaces. We find the very large inward relaxation of the surface Al atoms in the Al-terminated stoichiometric Al_2O_3 surface and the little outward relaxation of the surface O atoms in the O-terminated O-rich Al_2O_3 surface, as has been reported previously. On the contrary, the Ni surfaces show a slight atomic relaxation. The W_{sep} is appropriate for analysing fracture, where the bond separation rate is so quick that the surface cannot relax to ground state before the bonds rupture.

In order to reveal the adhesion nature of O-terminated and Al-terminated Ni/Al_2O_3 interfaces and reflect the different feature between them, we examine the charge redistribution after forming the stable interface from the initial Al_2O_3 and Ni surfaces having the same geometry as they have in the interface system. The charge redistribution, which is obtained by subtracting the superposed charge density of the separate Al_2O_3 and Ni surfaces from the Ni/Al_2O_3 charge density, can provide the rich knowledge for understanding the bonding nature of the interface. Figure 1 shows the charge redistributions for the O-terminated and Al-terminated Ni/Al_2O_3 interfaces. It can be seen that they have the quite different charge redistribution characteristics. Firstly, for the O-terminated interface, the obvious charge transfer and charge overlap between the interfacial O and Ni atoms are clearly shown in Fig.1(a). These characteristics indicate the existence of the strong ionic and O-2p/Ni-3d orbital hybridization interaction, respectively. This kind of interfacial charge transfer and orbital hybridization is observed also in the O-terminated Cu/Al_2O_3[20] and Nb/Al_2O_3 [17] systems. On the contrary, for the Al-terminated interface, the charge redistribution between the interfacial O and Ni atoms is rather weak, which indicates that there is not strong Ni–O bonding within the interface. This point is similar to the Al-terminated Cu/Al_2O_3 interface.[20] Secondly, it can be found that, for the Al-terminated interface, the presence of the interfacial Al atoms causes the peculiar charge redistribution within the interface Ni layer. There exist the charge accumulation and charge depletion in the two regions above the interfacial Al atom and around the Ni atom, respectively. This feature is consistent with that derived from the image-interaction model. Similar charge

redistribution is observed also in the Al-terminated Cu/Al_2O_3[20] and non polar metal/MgO[33] interfaces. Namely, due to the positive and negative charge associated with the Al and O ions in Al_2O_3, the corresponding charge accumulation and depletion distributions in the interfacial Ni layer can be deemed to play a role of screening. This electrostatic attractive interaction, which derived from the positive and negative charge pairs, is expected to be beneficial to the interfacial adhesion. However, as the most important result in this paper, we will verify that, for the Al-terminated Ni/Al_2O_3 interface, besides the electrostatic interaction, there should be the substantial hybridization interaction between the interfacial Ni and Al atoms.

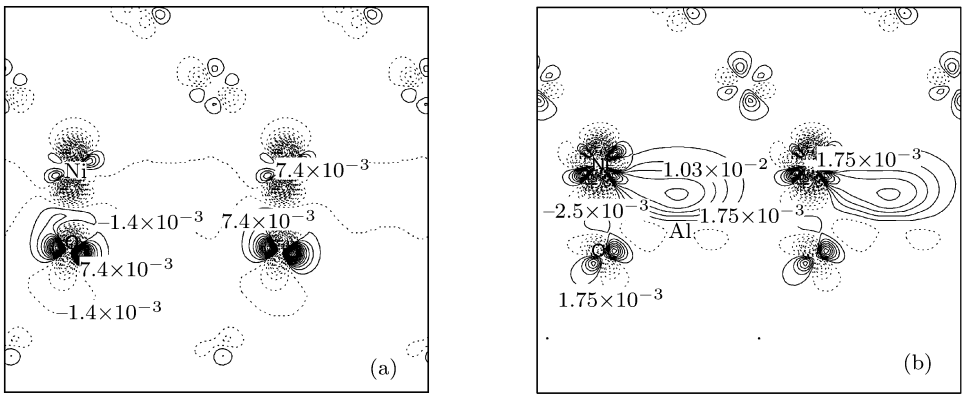


Fig.1. The redistributed charge through Al, O and Ni atoms due to adhesion for (a) O-terminated and (b) Al-terminated $Ni(111)/Al_2O_3(0001)$ interfaces. Positive contours (solid lines) denote charge accumulation due to adhesion and negative contours (dotted lines) indicate charge depletion. In (a), contours of the valence electron density are plotted from –0.24a.u.$^{-3}$ to 0.14a.u.$^{-3}$ with a spacing of 0.0088a.u.$^{-3}$. In (b), contours of the valence electron density are plotted from –0.13a.u.$^{-3}$ to 0.04a.u.$^{-3}$ with a spacing of 0.0043a.u.$^{-3}$.

Figure 2(a) shows the layer local density of states (LDOS) of the separate Al_2O_3 surface, which has the same geometry as it has in the stable Al-terminated Ni/Al_2O_3 interface. It is clearly seen that, besides exhibiting the band structure feature similar to bulk Al_2O_3, some additional peaks appear in the middle of the band gap, which we called as the gap states here. Correspondingly, the real spatial distribution of these gap states is plotted in Fig.2(b). It should be emphasized that these gap states, as presented in our preceding paper,[20] originate mostly from the dangling bonds of the surface Al atoms and are situated in the same region associated with the accumulated charge redistribution in Fig.1(b). However, in the LDOS of the stable Al-terminated Ni/Al_2O_3 interface, as shown in Fig.3, there are not the gap peaks similar to those

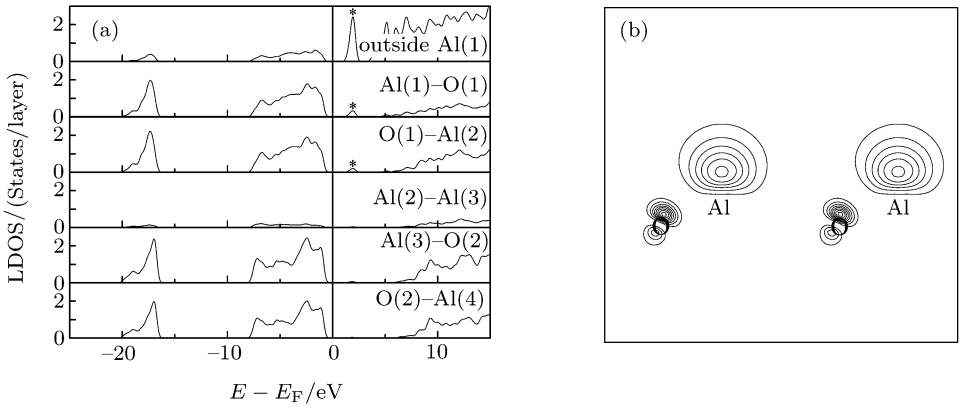


Fig.2. The gap states in (a) the LDOS and (b) real space for the separate $Al_2O_3(0001)$ surface. The asterisks and vertical line represent the gap states and the Fermi level, respectively. Al(n) and O(n) indicate the nth atomic layers towards the surface.

in the case of the Al_2O_3 surface. On the other hand, similarly to the Fig.2(b), Fig.4 shows the charge density associated with the eigenstates ranging from −2 eV to the Fermi level in Fig.3. It is really demonstrated that there exists some Ni–Al orbital hybridization. Thus, it can be said that it is just the hybridization interaction between the Ni orbitals and Al surface orbitals that results in the disappearance of the additional peaks, which come essentially from the dangling bonds of the surface Al atoms of the separate Al_2O_3 surface as shown in Fig.2(a). Simultaneously, accompanying this hybridization interaction, there seems to exist a charge increase in the interface region just above the Al site where Ni–Al hybridization may occur. This phenomenon is also observed in the Al-terminated Cu/Al_2O_3 interface.

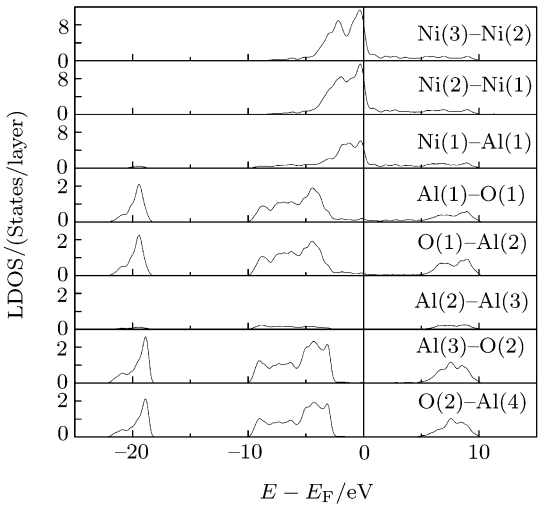


Fig.3. LDOS of the stable Al-terminated $Ni(111)/Al_2O_3$ (0001) interface. Al(n), O(n) and Ni(n) indicate the nth layers from the interface. The vertical line represents the Fermi level.

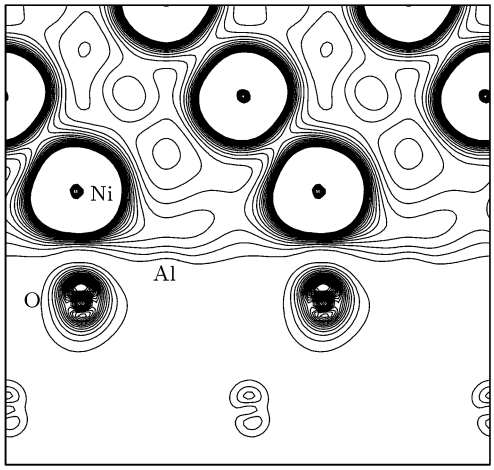


Fig.4. Spatial representation of the eigenstates ranging from –2 eV to the Fermi level associated with the LDOS in Fig.3. Contours of charge density are plotted from 0.002a.u.$^{-3}$ to 0.04a.u.$^{-3}$ with a spacing of 0.002a.u.$^{-3}$

In order to get further insight to the interfacial adhesion nature, we examine the direction among $\delta\rho(z)$ of charge transfer through the interface by plotting the one dimensional charge-transfer profile, as shown in Fig.5. It can be seen that the noticeable charge redistribution mainly involve two or three layers of the interface region. The charge density with both the bulk Al_2O_3 and Ni seems relatively unaffected by the interactions at the interface. By performing the integration of $\delta\rho(z)$ along the z axis from the outermost layer to the interface plane, we find that the physical charge transfer, for the O-terminated interface, is 0.414 e from Ni to Al_2O_3, suggesting the strong bonding between Ni and O atoms with both ionic and covalent appearance. The physical charge transfer for the Al-terminated interface is 0.256 e from Al_2O_3 to Ni, which is in contrast to the O-terminated case. The charge transfer primarily occurs from the underlying Al-O bond and O layers to the interface region just above the surface Al sites, where there may exist the Ni–Al hybridization. This indeed indicates that the interfaces possess the larger charge transfer quantity and consequent stronger adhesion nature, respectively. This can be understood from the nature of Ni with an unoccupied portion of d bands. The valence electron configurations of Ni and Cu atoms are $3d^84s^2$ and $3d^{10}4s^1$, respectively. Resultantly, their antibonding orbitals are only partially occupied and are fully occupied. On the other hand, it is well known from the most elementary principles of chemical bonding that the occupation of antibonding orbitals tends to cancel the effects of occupied bonding orbitals, and reduces the net chemical bonding strength in comparison with the situation where only bonding orbitals

are occupied. Moreover, it can be seen from Fig.3 that the interface dipole, which is generated by the charge transfer, shifts the LDOS of the Al_2O_3 bulk region toward the lower energies relative to the Fermi level E_F.

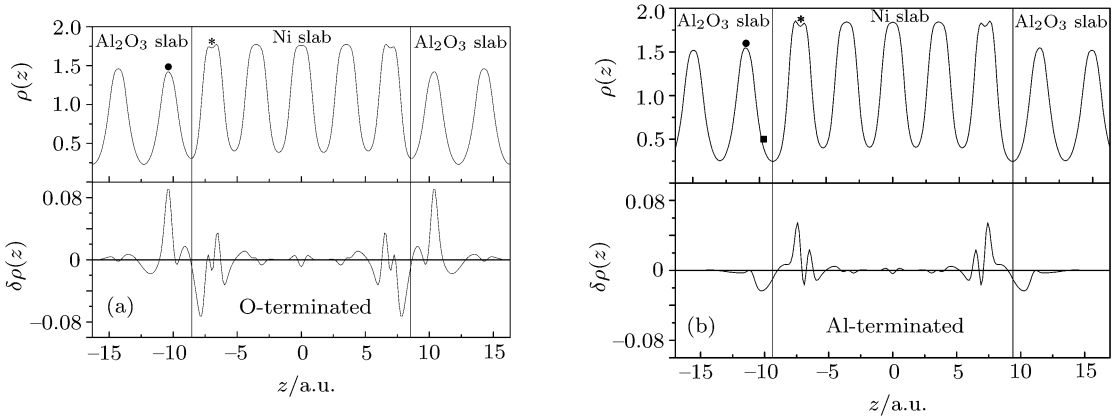


Fig.5. Planar-average valence electron density profile $\rho(z)$ and charge-transfer profile $\delta\rho(z)$ for (a) O-terminated and (b) Al-terminated Ni(111)/Al_2O_3(0001) interfaces. $\delta\rho(z)$= $\rho(z)$-$\rho_s(z)$, where $\rho_s(z)$ is the superposition of the planar-averaged charge densities of the separate Ni and Al_2O_3 surfaces. The interface plane is denoted by vertical lines, where $\rho(z)$ is a minimum between the interfacial Ni and O or Al atoms. A closed circle, a closed square and an asterisk indicate the positions of the interface O(1), Al(1) and Ni(1) atomic layers as labelled in Figs.2(a) and 3, respectively.

Of course, it is not straightforward to differentiate between the image-like electrostatic and orbital hybridization contributions to the Al-terminated Ni/Al_2O_3 interface bonding, because the charge redistribution induced by these two interactions cannot be demonstrably separated. However, using the same method as adopted in our previous work about the Cu/Al_2O_3 interface, it is possible to make a rough estimate about the relative magnitude of these two components.

As mentioned above, in the process that the separate Al-terminated stoichiometric Al_2O_3 surface relaxes into the free surface, the surface Al atoms exhibit a large inward drop. Together with this drop, the gap peaks in the LDOS will approach the bottom of the conduction band. Based on this point, we try to construct a rigid interface by artificially combining the relaxed free Al-terminated stoichiometric Al_2O_3 surface with the unrelaxed separate Ni surface, having the same atomic positions as in the stable interface. At this time, it is found that the corresponding charge transfer in this rigid interface is 0.212 e, which is less than that (0.256 e) in the stable interface. This suggests that the Ni–Al hybridization is weaker than that in the stable interface.

According to the definition in Section 2, the W_{sep} of the rigid interface can be obtained, as shown in Table 2. It should be noted that the separated Al_2O_3 surface in this case corresponds to the relaxed free Al_2O_3 surface. For the purpose of clarity, in parentheses in Table 2, we also list the W_{sep} of the rigid interface with regard to the same separate Al_2O_3 and Ni surfaces as those for the calculation of W_{sep} of the stable interface. We know that the energy gain, in forming the stable interface from the two separate surfaces, is 2.387J/m^2, which includes both the image-like electrostatic and Ni–Al orbital hybridization contributions. This stable interface is then changed into the rigid interface by relaxing the configuration of the interfacial Al_2O_3 region, which causes an increase in energy of 0.695J/m^2, so that the rigid interface has an energy gain of 1.692J/m^2 relative to the same separate surfaces as associated with the stable interface. On the other hand, in general, the image-like electrostatic interaction seems not to depend so much on the interface configuration. Hence energy loss of 0.695J/m^2 should be mainly attributable to the weakening of the hybridization. It is worthwhile to mention that this value is about one quarter of 2.387J/m^2, being substantial in comparison with the total separation or adhesive energy. Of course, even in the rigid interface, there exist both the image-like electrostatic and orbital hybridization interactions, because the reduction in the charge transfer is only small. Therefore, we can draw a conclusion that the hybridization interaction between interfacial Ni and Al atoms is substantial and cannot be neglected.

Table 2. Work of separation, W_{sep}, work of adhesion, W_{ad}, and charge transfer for rigid and stable Al-terminated Ni(111)/Al_2O_3(0001) interfaces. Results of the Cu(111)/Al_2O_3(0001) interface (Ref.[20]) are also listed.

	$W_{sep}/(J/m^2)$	$W_{ad}/(J/m^2)$	charge transfer/e
Al-terminated Ni(111)/Al_2O_3(0001) interface			
stable interface	2.387	1.828	0.256
rigid interface	1.192 (1.692)	1.134	0.212
Al-terminated Cu(111)/Al_2O_3(0001) interface			
stable interface	1.62	1.27	0.18
rigid interface	0.87 (1.19)	0.84	0.15

4. Conclusion

The Ni(111)/Al_2O_3(0001) interface has been studied by using the first-principles pseudopotential method. It is found that the interface stoichiometry is of great importance to the interfacial properties. The O-terminated and Al-terminated interfaces have quite different features. The Ni–O bond at the O-terminated interface has the strong ionic and O-2p/Ni-3d orbital hybridization characters. The bonding strength of the Al-terminated interface is weak, containing the image-like electrostatic and the Ni–Al orbital hybridization interactions, and the latter is substantial and cannot be neglected. The interfacial charge transfer induced by the Ni–Al orbital hybridization interaction occurs from Al_2O_3 to Ni, which is opposite to that in the O-terminate interface.

References

[1] Henrich V E and Cox P A 1994 *The Surface Science of Metal Oxides* (Cambridge: Cambridge University Press) p112
[2] French R H and Heuer A H 1994 *J. Am. Ceram. Soc.* **77** 292
[3] Gautier M, Fenaud G, Van L P, Villette B, Pollak M, Thromat N, Jollet F and Duraud J P 1994 *J. Am. Ceram. Soc.* **77** 323
[4] Kumar D, Pennycook S J, Lupini A, Duscher G, Tiwari A and Narayan J 2002 *Appl. Phys. Lett.* **81** 4204
[5] Wang S C and Wei W C J 2003 *J. Mater. Res.* **18** 1566
[6] Costina I and Franchy R 2001 *Appl. Phys. Lett.* **78** 4139
[7] Chatain D, Coudurier L and Eustathopoulos N 1988 *Rev. Phys. Appl.* **23** 1955
[8] Merlin V and Eustathopoulos N 1995 *J. Mater. Sci.* **30** 3619
[9] Brydson R, Muullejans, Bruley J, Trusty P A, Sun X, Yeomans, J A and Ruhle 1995 *J. Micros.* **177** 369
[10] Zhong Q and Ohuchi F S 1990 *J. Vac. Sci. Technol.* A **8** 2107
[11] Chatterjee A, Niwa S and Mizukami F 2005 *J. Mol. Graph.* **23** 447
[12] Finnis M W 1992 *Acta Metall. Mater.* **40** S25
[13] Finnis M W 1996 *J. Phys.-Condes. Matter* **8** 5811
[14] Zhao G L, Smith J R, Raynolds J and Srolovitz D J 1996 *Interface Sci.* **3** 289
[15] Batyrev I G, Alavi A, Finnis M W and Deutsch T 1999 *Phys. Rev. Lett.* **82** 1510
[16] Smith J R and Zhang W 2000 *Acta Mater.* **48** 4395
[17] Zhang W and Smith J R 2000 *Phys. Rev.* B **61** 16883
[18] Zhang W and Smith J R 2000 *Phys. Rev. Lett.* **85** 3225
[19] Zhang W, Smith J R and Evans A G 2002 *Acta Mater.* **50** 3803
[20] Yang R, Tanaka S and Kohyama M 2004 *Phil. Mag. Lett.* **84** 425
[21] Batyrev I G and Kleinman L 2001 *Phys. Rev.* B **64** 033410
[22] Johnson K H and Pepper S V 1982 *J. Appl. Phys.* **53** 6634
[23] Anderson A B, Methandru S P and Smialek J L 1985 *J. Electrochem. Soc.* **132** 1695
[24] Zdetisis A D and Kunz A B 1985 *Phys. Rev.* B **32** 6358
[25] Raatz F and Salahub D R 1985 *Surf. Sci.* **156** 982
[26] Zhang J M, Huang Y H, Xu K W and Ji V 2007 *Chin. Phys.* **16** 210
[27] Jin Y J, Lin J B and Lee J I 2007 *Chin. Phys.* **16** 506
[28] Zhang Y, Lü G H, Deng S H and Wang T M 2006 *Acta Phys. Sin.* **55** 2901 (in Chinese)
[29] Zhang J M, Wei X M, Xin H and Xu K W 2005 *Chin. Phys.* **14** 1015
[30] Lao Y F and Wu H Z 2005 *Acta Phys. Sin.* **54** 4334 (in Chinese)
[31] Blöchl P, Das G P, Fishcmeister H F and Schönberger U 1989 *Metal-Ceramic Interfaces* (Oxford: Pergamon) p9
[32] Smith J R, Hong T and Srolovitz D J 1994 *Phys. Rev. Lett.* **72** 4021
[33] Hong T, Smith J R and Srolovitz D J 1994 *J. Adhes. Sci. Technol.* **8** 837
[34] Kruse C, Finnis M W, Lin J S, Payne M C, Milman V Y, Vita A De and Gillan M J 1996 *Phil. Mag. Lett.* **73** 377
[35] Perdew J P and Zunger A 1981 *Phys. Rev.* B **23** 5048
[36] Tamura T, Lu G H, Yamamoto R, Kohyama M, Tanaka S and Tateizumi Y 2004 *Model. Simul. Mater. Sci. Eng.* **12** 945
[37] Kresse G and Furthmüller J 1996 *Phys. Rev.* B **54** 11169
[38] Pulay P 1980 *Chem. Phys. Lett.* **73** 393
[39] Troullier N and Martins J L 1991 *Phys. Rev.* B **43** 1993
[40] Kleinman L and Bylander D M 1982 *Phys. Rev. Lett.* **48** 1425
[41] Saiz E, Cannon R M and Tomsia A P 1999 *Acta Mater.* **47** 4209